Comparison of a SiO2-CaO-ZnO-SrO Glass Polyalkenoate Cement to Commercial Dental Materials: Glass Structure and Physical Properties

A. W. Wren

A. Coughlan

F. R. Laffir

Mark R. Towler
Missouri University of Science and Technology, mtowler@mst.edu

Recommended Citation

Comparison of a SiO$_2$–CaO–ZnO–SrO glass polyalkenoate cement to commercial dental materials: glass structure and physical properties

A. W. Wren · A. Coughlan · F. R. Laffir ·
M. R. Towler

Abstract Glass polyalkenoate cements (GPCs) have previously been considered for orthopedic applications. A Zn–GPC (BT 101) was compared to commercial GPCs (Fuji IX and Ketac Molar) which have a setting chemistry analogous to BT 101. Handling properties (working, T_w and setting, T_s times) for BT 101 were shorter than the commercial GPCs. BT 101 also had a higher setting exotherm (S_x —34 °C) than the commercial GPCs (29 °C). The maximum strengths for BT 101, Fuji IX, and Ketac Molar were 75, 238, and 216 MPa (compressive, σ_c), and 34, 54, and 62 MPa (biaxial flexural strengths, σ_f), respectively. The strengths of BT 101 are more suitable for spinal applications than commercial GPCs.

1 Introduction

Conventional glass polyalkenoate cements (GPCs) were introduced in 1972 by Wilson and Kent and are commercially used in dental restorative applications. Glass polyalkenoate cements primarily consist of a polyalkenoic acid, typically polyacrylic acid (PAA) and a fluoro-alumino-silicate based glass [1–3]. Upon mixing, an acid–base reaction occurs resulting in metal ions from the glass (e.g. strontium, aluminium, calcium) forming a polyacid salt with carboxylate (COO$^-$) groups from the PAA resulting in a hard set material. The glass particulate surface subsequently forms a silica hydrogel and any unreacted cores of the glass particles remain in the cements as inorganic fillers [1]. Additional advantages of using GPCs in dental applications include fluoride (F) release which has been cited to have anti-cariostatic properties [1, 4, 5]. They are also aesthetically suitable [5], have a low setting exotherm [6], and have minimal shrinkage upon setting[7].

In recent years, GPCs have been employed for use in orthopedics. These applications include ear, nose, and throat surgery where GPCs have been used to cement cochlea implants, seal imperfections in the skull, and to create prefabricated ossicies [8]. Glass polyalkenoate cements are specifically tailored for applications in close proximity to hard biological materials such as tooth enamel and dentin, which consists predominantly of tightly packed hydroxy-apatite (HA) crystals forming a microporous structure [3, 9]. Glass polyalkenoate cements have a number of advantages in close proximity to HA such as a close chemical bond which is achieved through ionic exchange at the interface. Polyacrylic acid chains can enter the molecular surface of HA replacing a concentration of calcium and phosphate ions. Subsequent ion exchange between the GPC and COO$^-$ groups from the PAA chain forms a strong acid/base resistant interfacial layer [1, 5]. Glass polyalkenoate cements have been employed in orthopedics to reinforce osteoporotic femoral heads to improve the stability of hip screws [8]. However, complications related to Aluminium (Al^{3+}) exposure have been problematic [10, 11], as there is anecdotal evidence that Al contributes to neurological disorders [12, 13] and negatively

A. W. Wren (✉) · A. Coughlan
Inamori School of Engineering, Alfred University, Alfred,
NY 14802, USA
e-mail: wren@alfred.edu

F. R. Laffir
Materials and Surface Science Institute, University of Limerick,
Limerick, Ireland

M. R. Towler
Department of Biomedical Engineering, University of Malaya,
Kuala Lumpur, Malaysia

M. R. Towler
Department of Mechanical & Industrial Engineering,
Ryerson University, Toronto, Canada

alters the mineralization of skeletal tissue [14]. However, Al in the glass phase of conventional GPCs provides an important structural role where it partly replaces the silica inducing negative sites which are charge compensated by sodium (Na^+), strontium (Sr^{2+}) or calcium (Ca^{2+}) [15]. Setting of GPCs also involve cross-linking of the polyacid with Al^{3+} (and M^{2+}) which form stable Al–PAA complexes during setting [15, 16].

This study sees the development of a zinc (Zn)-based GPC designed for orthopedic spinal applications, where this material would be in close contact with mineralized trabecular bone and soft tissues. For this reason, the constituents of this novel GPC have been included to encourage bone growth and development [17, 18]. Zinc ions has been described as having a positive effect on bone metabolism, having antibacterial properties [19–21] and is a prevalent ion in the body. Strontium (Sr^{2+}) is also known to have a positive effect on bone metabolism where it increases the differentiation of pre-osteoblasts while simultaneously decreasing osteoclastic activity, resulting in a positive shift in the rate of bone turnover [22, 23]. For this work, Zn^{2+} is substituted for Al^{3+} in the glass phase as they both act as network intermediates, however, Zn^{2+} is regarded as being a more biologically acceptable ion. This study looks at developing a Zn–GPC with physical properties that are more comparable for use in spinal surgery by altering the starting glass composition. Fuji IX and Ketac Molar cements were chosen for comparison as they are commonly used commercial materials and experience similar setting and maturation chemistry to the experimental GPC under investigation.

2 Materials and methods

2.1 Experimental materials

BT 101—Experimental GPC: A 0.12Ca–0.04Sr–0.36Zn–0.48Si glass (BT 101) was formulated by weighing out appropriate amounts of analytical grade reagents (Sigma-Aldrich, Dublin, Ireland) and ball milling (1 h). The mix was then oven dried (100 °C, 1 h) and fired (1,500 °C, 1 h) in a platinum crucible and shock quenched into water. The resulting frit was dried, ground, and sieved to retrieve a glass powder with a maximum particle size of 45 μm.
  Fuji IX—GC Co. Japan (#0508291).
  Ketac Molar—ESPE/3 Dental, MN, USA (#224927).

2.2 Glass characterization

2.2.1 X-Ray diffraction (XRD)

Diffraction patterns were collected using a Philips Xpert MPD Pro 3040/60 X-ray Diffraction Unit (Philips, Netherlands).

Disc samples (32 mm Ø × 3 mm) were prepared by pressing a selected glass powder (<45 μm) into a backing of ethyl cellulose (8 tonnes, 30 s). Samples were then placed on spring-back stainless steel holders with a 10 mm mask and were analyzed using Cu Kα radiation. A generator voltage of 40 kV and a tube current of 35 mA were employed. Diffractograms were collected in the range $5° < 2\theta < 80°$, at a scan step size $0.008\overset{\circ}{3}$ and a step time of 10 s. Any crystalline phases present were identified using JCPDS (Joint Committee for Powder Diffraction Studies) standard diffraction patterns.

2.2.2 Particle size analysis (PSA)

Particle size analysis was achieved using a Coulter Ls 100 Fluid module Particle size analyzer (BeckmanCoulter, Fullerton, CA, USA). The glass powder samples were evaluated in the range of 0.375 – 948.2 μm and the run length took 60 s. The fluid used in this case was glycerol and was used at a temperature range between 10 and 37 °C. The relevant volume statistics were calculated on each glass.

2.2.3 Differential thermal analysis (DTA)

A combined differential thermal analyser–thermal gravimetric analyser (DTA–TGA) (Stanton Redcroft STA 1640, Rheometric Scientific, Epsom, UK) was used to measure the glass transition temperature (T_g) for each glass. A heating rate of 20 °C/min^{-1} was employed using an air atmosphere with alumina in a matched platinum crucible as a reference. Sample measurements were carried out between 30 and 1,000 °C.

2.2.4 Network connectivity (NC)

The network connectivity of the BT 101 glass was calculated (Eq. 1) using the molar compositions of the glass. Network connectivity calculations were performed assuming that Zn performs as a network modifier.

$$NC = \frac{No.BOs - No.NBOs}{Total\ No.\ Bridging\ Species} \quad (1)$$

where BO is bridging oxygen and NBO is non-bridging oxygen.

2.2.5 X-ray photoelectron spectroscopy (XPS)

X-ray Photoelectron Spectroscopy was performed in a Kratos AXIS 165 spectrometer (Kratos Analytical, Manchester, UK) using monochromatic Al Kα radiation (hυ = 1,486.6 eV). Surface charging was minimized by flooding the surface with low energy electrons. The C 1 s peak of adventitious carbon at 284.8 eV was used as a charge reference to calibrate the binding energies. High

resolution spectra were taken at pass energy of 20 eV, with step size of 0.05 eV and 100 ms dwell time.

2.3 Handling and thermal properties

2.3.1 Cement preparation

BT 101—Cements were prepared by thoroughly mixing the glass powders (<45 μm) with E9 (PAA—Mw, 80,800, Advanced Healthcare Limited, Kent, UK) and distilled water on a glass plate. The cements were formulated at a P:L ratio of 2:1.5 with 50 wt% additions of PAA, where 1 g of glass powder was mixed with 0.37 g E9 PAA and 0.37 ml water. Complete mixing was undertaken within 20 s. Fuji IX (P:L—3.6:1.0) & Ketac Molar (P:L—4.5:1.0)—Appropriate quantities were used to fill moulds and preparation of cements was completed in accordance with the manufacturer's instructions. Each material was hand-mixed using a clean glass plate and spatula.

2.3.2 Handling properties

The setting times (T_s, where $n = 3$) of the cement series were tested in accordance with ISO9917 which specifies the standard for dental water-based cements [24]. The working time (T_w, where $n = 3$) of the cements was measured under standard laboratory conditions (Ambient Temp, $A_T \sim 25$ °C), and was defined as the period of time from the start of mixing during which it was possible to manipulate the material without having an adverse effect on its properties. Each sample was measured using a stopwatch on a clean glass plate with a sterile spatula. Each measurement was conducted under the same mixing conditions to ensure reproducibility.

2.3.3 Exotherm determination

Plastic moulds (12.6 mm height, 12.5 mm Ø) were filled with cement (n = 3) in order to determine the peak setting exotherm (S_x). A thermocouple attached to an Accumet portable AP6 multimeter (Reagecon, Shannon, Ireland) was placed into the cement 30 s after mixing commenced and the peak exotherm was recorded directly from the meter. Each reading was conducted at ambient laboratory temperature (Ambient Temp, $A_T \sim 25$ °C) using a stopwatch and sterile spatula.

2.4 Mechanical properties

2.4.1 Compressive strength

The compressive strengths (σ_c) of the cements (where $n = 5$) were evaluated in accordance with ISO9917 [24]. Cylindrical samples measuring (6 × 4 mm Ø) were tested after 1, 7, 30, and 90 days. Samples were stored in sterile de-ionized water in an incubator at 37 °C. At each time period, the cements were removed and tested while wet on an Instron 4082 Universal Testing Machine (Instron Ltd., High Wycombe, Bucks, UK) using a 5 kN load cell at a crosshead speed of 1 mm/min^{-1}. The σ_c was calculated using Eq. 2.

$$C = \frac{4\rho}{\pi d^2} \tag{2}$$

where ρ is maximum applied load (N), d is diameter of sample (mm)

2.4.2 Biaxial flexural strength

The biaxial flexural strength (σ_f) of the cements (where $n = 5$) were evaluated by a method described by Williams et al. [25]. Cement discs measuring (2 × 12 mm Ø) were tested after 1, 7, 30, and 90 days. Samples were stored in sterile deionized water in an incubator at 37 °C. At each time period, the cements were removed and tested while wet on an Instron 4082 Universal Testing Machine (Instron Ltd., High Wycombe, Bucks, UK) using a 1 kN load cell at a crosshead speed of 1 mm/min^{-1}. The σ_f was calculated using Eq. 3.

$$\text{BFS} = \frac{\rho(N)}{t^2}\{0.63\ln(r/t) + 1.156\} \tag{3}$$

where ρ is maximum applied load (N), t is thickness of sample (mm), r is radius of support diameter (mm).

2.4.3 Biaxial flexural modulus

The biaxial flexural modulus (E_f) was calculated in accordance with a publication by Higgs et al. [26]

$$\frac{dP}{d\omega_c} = \frac{Eh^3}{\beta_c a^2} = E\left(\frac{h^3}{\beta_c a^2}\right) \tag{4}$$

where $\frac{dy}{d\omega_c}$ = load displacement slope of the flexural test data. a is radius of the support points, h is thickness of the disc, E is flexural modulus, β_c is center of deflection function.

2.4.4 Hardness testing

A number of indents were measured for each material (BT 101, Fuji IX and Ketac Molar) at each time period (1, 7, 30 and 90 days). Three cement discs per individual cement were used at each time period with ten indents being recorded per disc. This resulted in $n = 30$ indents measured per cement sample at each time period. Each cement disc was mounted in epoxy resin and polished using 600 grit silicon carbide polishing paper. Ten Vickers indentations at a load of 500 g

and a dwelling time of 15 s were made to each disc using a universal hardness machine (HMV-200, Shimadzu, MD, USA). Using the attached light microscope and computer, the diagonals created by the Vickers diamond indenter were measured and the VHN was calculated using Eq. 5.

$$Hv = 1.854 \frac{F}{d^2} \qquad (5)$$

where F is the applied load (kgf), d is diagonal length (mm).

2.5 Statistical analysis

One-way analysis of variance (ANOVA) was employed to compare the mechanical properties of the materials in relation to 1) maturation and 2) between materials at each time period. Comparisons of relevant means were performed using the post hoc Bonferroni test. Differences between groups was deemed significant when $P \leq 0.05$.

3 Results

3.1 Glass characterization

X-ray diffraction (XRD) determined that BT 101 (Fig. 1) exhibited a number of crystalline phases including Quartz (SiO_2, 04-008-7653), Zinc Silicate ($Zn_{1.7}SiO_4$, 00-024-1466), SiO_2 (00-029-0085), and Zincite (ZnO, 04-003-2106) however, the characteristic amorphous hump is also present. Diffraction patterns of Fuji IX exhibits amorphous characteristics while Ketac Molar exhibits crystalline species which includes Calcium Lanthanum Fluoride ($Ca_{0.62}La_{0.38}F_{2.38}$, 04-007-6893). An additional single peak is present at 29 °2 theta which can be attributed to either Ca or La_2O_3. Table 1 shows the composition of each glass as determined by **X-ray photoelectron spectroscopy (XPS)**. The Si content was found to be highest in BT 101 (55 at%) when compared to Fuji IX (18 at%) and Ketac Molar (33 at%). Both Fuji IX and Ketac Molar had similar aluminum (Al), 13.7 and 19.3 at%, fluorine (F), 30.1 and 39.3 at%, phosphate (P), 3.2 and 3.0 at%, and sodium (Na), 2.6 and 3.8 at% concentrations, respectively. Fuji IX also contained strontium (Sr), 11.5 at% and titanium (Ti), 2.9 at%, while Ketac Molar contained lanthanum (La), 5.6 at% and calcium (Ca) 11.9 at%. The **network connectivity (NC)** of BT 101 was found to be 1.83, which correlates with MAS–NMR data on this glass [27]. The NC of Fuji IX and Ketac Molar were reproduced from previous studies by Stamboulis et al. assuming the aluminum is Al(IV), there is local charge compensation of Al^{3+} and P^{5+} and that fluorine forms non-bridging fluorine's. It was determined that the NC of Fuji IX and Ketac Molar were 3.48 and 2.41, respectively [28]. **Differential thermal**

analysis (DTA) was employed to determine the glass transition temperature (T_g) for each material and is presented in Fig. 2a. The T_g was found to be 670 °C for BT 101, 565 °C for Fuji IX, and 430 °C for Ketac Molar. Figure 2b shows **particle size analysis (PSA)** of each glass. BT 101 had a slightly higher d (0.1) than either Fuji IX or Ketac Molar at 44 μm compared to 14 and 9 μm, respectively. d(0.5) was also higher for BT 101 at 13 μm while Fuji IX and Ketac Molar were 4 and 3 μm, respectively. For d(0.9), each glass had similar size fine particles, 1.4 μm (BT 101), 1.2 μm (Fuji IX), and 1.1 μm (Ketac Molar).

3.2 Handling and thermal properties

Both the working times (T_w) and setting times (T_s) are presented in Fig. 3a. The T_w of BT 101 was found to be 20 s while the T_w of Fuji IX and Ketac Molar was 126 and 146 s, respectively. The T_s exhibited a similar trend where BT 101 presented a T_s of 45 s and Fuji IX and Ketac Molar presented a T_s of 196 and 179 s, respectively. Figure 3b shows the setting exotherm (S_x) of BT 101 compared to Fuji IX and Ketac Molar. The S_x of BT 101 was found to be 34 ± 1 °C ($A_T + 9$ °C) while the S_x of Fuji IX and Ketac Molar were found to be 29 ± 1 °C ($A_T + 4$ °C).

3.3 Mechanical properties

The **compressive strength (σ_c)** is presented in Fig. 4a, BT 101 attained σ_c ranging from 63 to 75 MPa over 1–90 days. Fuji IX and Ketac Molar exhibited higher σ_c strengths of 211–238 and 192–174 MPa over 1–90 days, respectively. **Biaxial flexural testing (σ_f)** was also conducted over the same time periods and is presented in Fig. 4b. BT 101 exhibited σ_f of 26–34 MPa over 1– 90 days. Fuji IX exhibited higher σ_f which ranged from 46 to 44 MPa over 1–90 days and Ketac Molar showed similar σ_f of 38–51 MPa over 1–90 days. The **biaxial flexural modulus (E_f)** was calculated for each material over 1, 7, 30, and 90 days (Fig. 5a). BT 101 exhibited E_f which ranged from 0.39 to 0.55 GPa over 1–90 days. Fuji IX exhibited much higher E_f which was found to increase at each time period. The E_f of Fuji IX was found to be 1.99 (1 day), 2.07 (7 days), 2.33 (30 days), and 2.76 GPa after 90 days. Ketac Molar presented a similar trend as Fuji IX where the E_f was found to be 1.76 (1 day), 2.91 (7 days), 3.03 (30 days), and 4.16 GPa after 90 days. Figure 5b shows the **hardness** testing over 1, 7, 30, and 90 days and is presented in Fig. 5b. BT 101 exhibited hardness values which decreased from 1.24 to 0.95 GPa over 1–90 days. Fuji IX exhibited hardness values that remained relatively constant, 0.83–0.75 GPa over 1–90 days. Ketac Molar exhibited a similar trend to Fuji IX where the hardness values were relatively constant over

Fig. 1 XRD patterns of GPCs glass phase
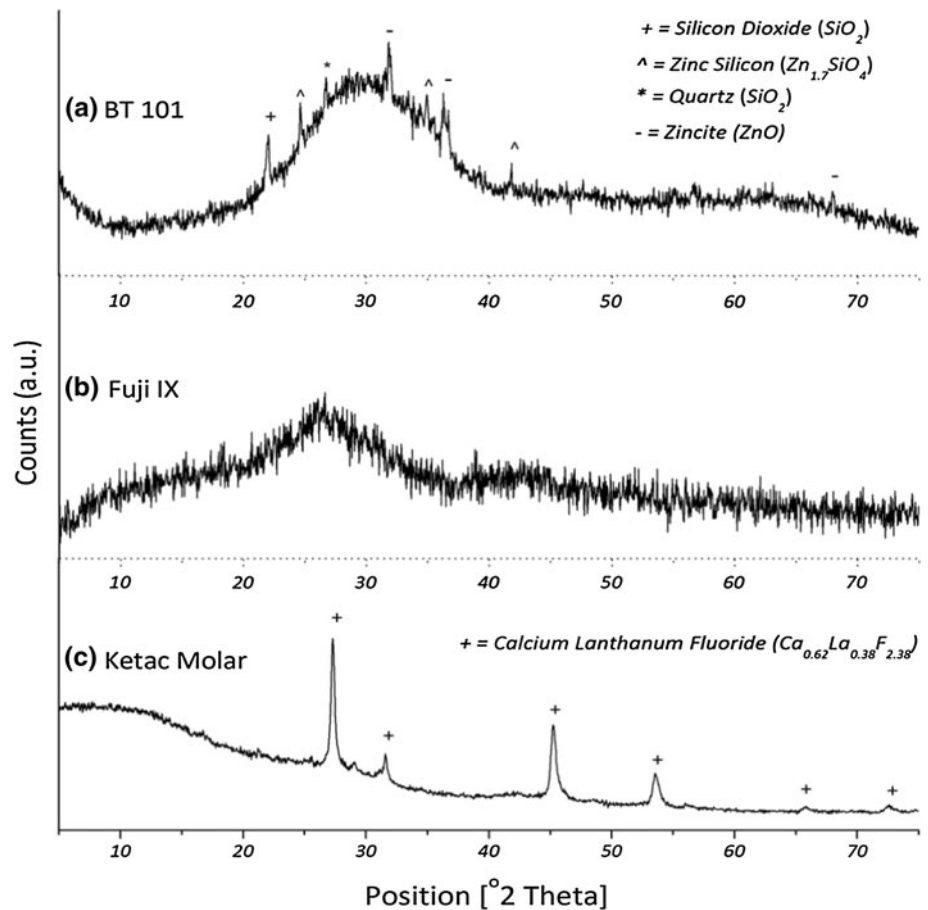
Table 1 Glass composition determined by XPS

	BT 101	Fuji IX	Ketac Molar
Si	55.3	18.3	32.8
Na	–	3.8	2.6
F	–	39.3	30.1
Al	–	19.3	13.7
P	–	3.0	3.2
La	–	–	5.6
Ca	11.3	–	11.9
Sr	4.1	11.5	–
Ti	–	4.9	–
Zn	29.3	–	–

1–30 days at 0.86–0.90 GPa, however, reduced to 0.54 GPa after 90 days.

4 Discussion

4.1 Glass characterization

X-ray diffraction (XRD) was performed to determine any structural differences present between the glass phase of the commercial glasses and the experimental SiO_2–CaO–ZnO–SrO glass (BT 101). The crystalline phases identified in the glass phase (Fig. 1) of Fuji IX and Ketac Molar here correlate well with previous studies on this glass [28]. X-ray photoelectron spectroscopy was employed to determine the relative difference in composition between each material and the results are presented in Table 1. The composition derived for BT 101 (Si, Ca, Zn, Sr) is intentionally very different to the composition of Fuji IX and Ketac Molar. The predominant difference in composition between the commercial glasses is the presence of Lanthanum (La, 5.6 at%) in Ketac Molar and strontium (Sr, 11.5 at%) in Fuji IX [29]. Both La and Sr assume similar roles in these materials where they act as a radiopacifier which allows for imaging under an X-ray source. The network connectivity (NC) of Fuji IX and Ketac Molar were found to be greater than BT 101 which is likely due to the presence of additional network forming oxides present in the commercial glasses. Aluminum (Al^{3+}) and Phosphorus (P^{5+}) provide additional network forming roles analogous to Silica (Si^{4+}) assuming they are sufficiently charge compensated by network modifiers present in the glass. Higher NC values suggest that the commercial glass phases have greater interconnectivity and consequently are

Fig. 2 **a** glass transition temperature and **b** particle size analysis of glasses
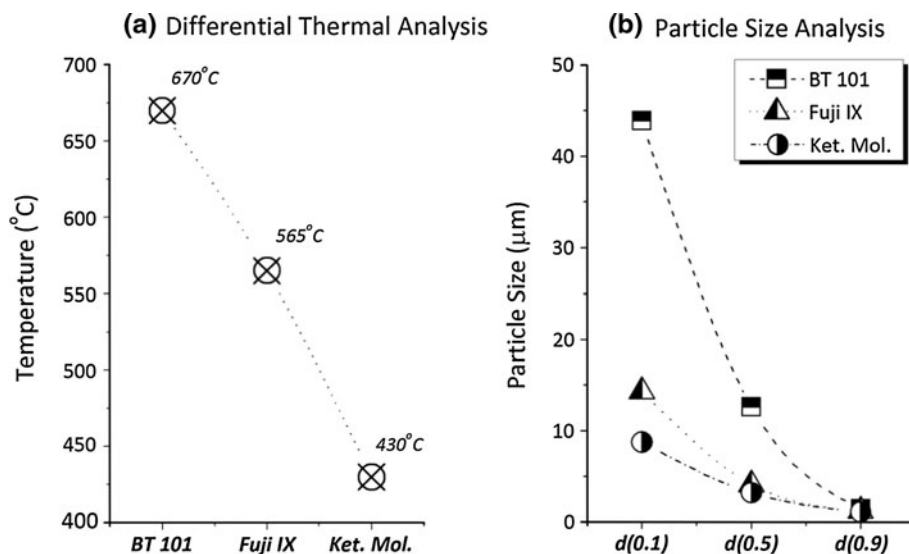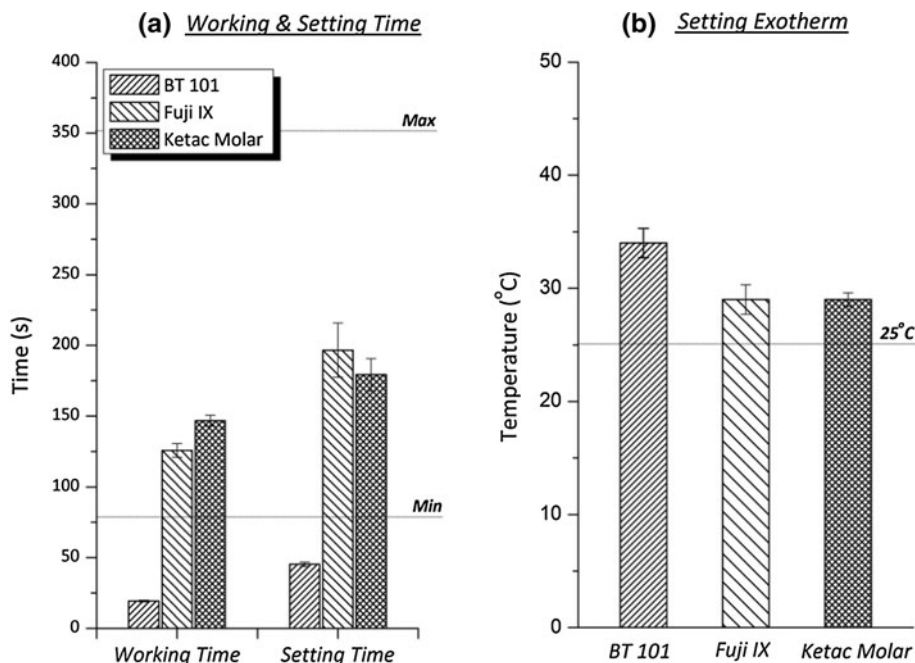

Fig. 3 **a** Working and setting times and **b** setting exotherm of GPCs

less soluble than the experimental BT 101 glass. Stamboulis et al. [28] suggests that the lower NC value attained for Ketac Molar (2.41) is responsible for amorphous phase separation within the glass and subsequently encourages the formation of crystal species. The lower NC attributed to BT 101 (1.83) exhibited a number of crystal species, however, the majority of the diffractogram represents a predominantly amorphous material. The T_g of each material is presented in Fig. 2a and it was found that the T_g of both Fuji IX (565 °C) and Ketac Molar (430 °C) were much lower than BT 101 (670 °C). The higher T_g attributed to BT 101 is likely due to the higher Si content present in BT 101, and the lower T_g determined in the commercial glasses is likely due to the high concentration of network

modifiers present. However, to accurately determine the relationship between the NC and T_g, characterization methods such as MAS–NMR/Raman spectroscopy would be required. Particle size analysis (PSA) is presented in Fig. 2b and it was found that BT 101 contained a higher concentration of d(0.1) and d(0.5) than the commercial glasses, which is likely due to the methods employed to grind the glass. d(0.9) was found to be similar for each glass.

4.2 Handling and thermal properties

The T_w and T_s (Fig. 3a) are important characteristics to consider when implanting viscous materials into the human

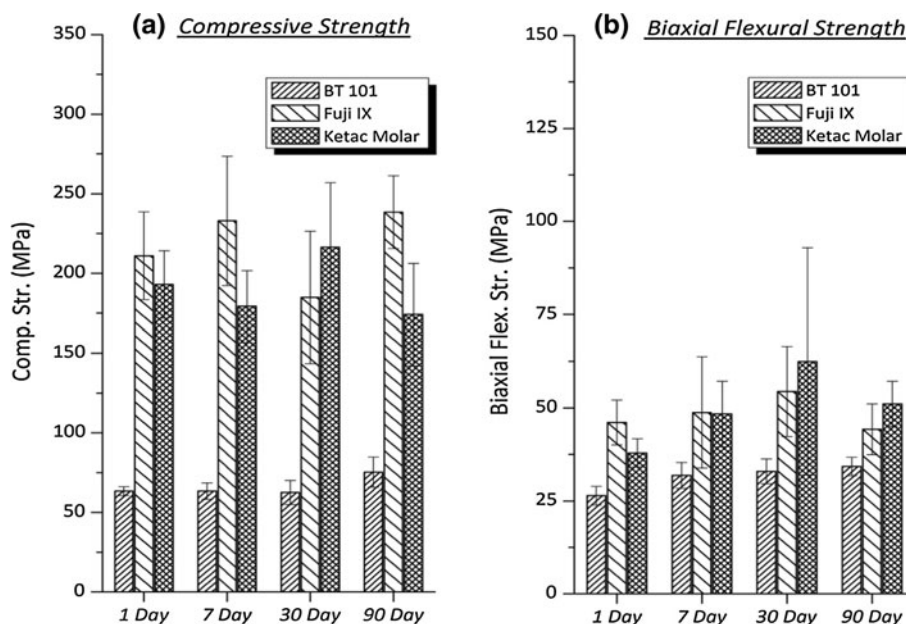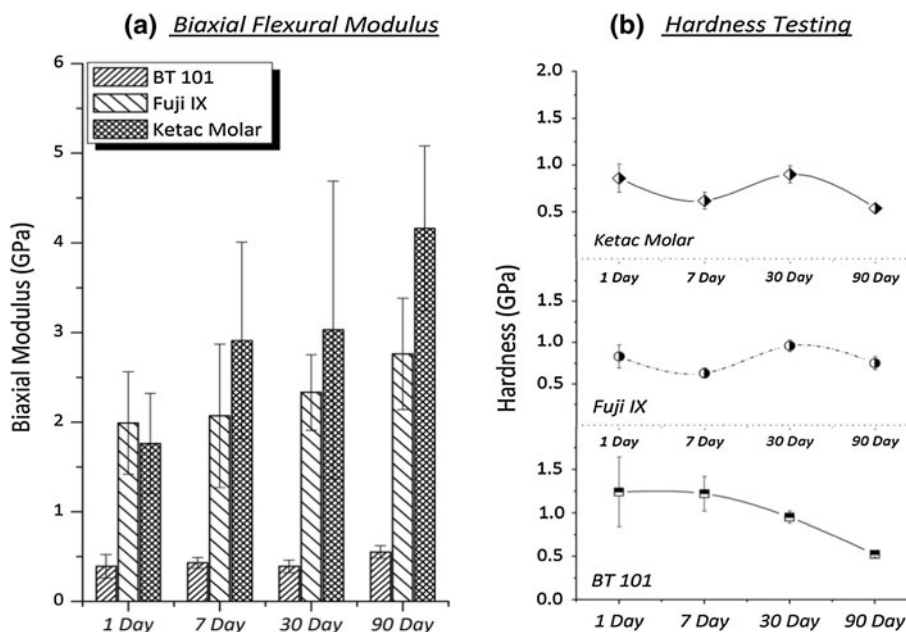**Fig. 4** **a** Compressive and **b** biaxial flexural strength of cement series

Fig. 5 **a** Biaxial flexural modulus and **b** hardness of cement series

body. Prolonged T_s can increase a patient's risk of septic complications which has been reported using PMMA, which have a T_s spanning 10–15 min [30]. The handling properties exhibited by BT 101 are not suitable for orthopedic applications as the cements set within 45 s, which may be attributed to an accelerated acid base setting reaction compared to the commercial materials. This is far shorter than the minimum requirements outlined by ISO standards [24]. Differences in the handling characteristics can be attributed to a number of factors. The glass particle size can have a significant effect, where smaller particles will have an increased surface area and will increase the particle dissolution rate of the finer glass particles [31]. The

solubility of the glass can be attributed to the ratio of network forming cations to network modifying cations [32], which influences non-bridging oxygen's (NBOs) formation. Non-bridging oxygens are known to promote solubility and facilitate ion release [32]. Also, higher M_w PAA will form cross-bridges with ions more rapidly than with lower M_w acids [33]. The use of tartaric acid in commercial materials alters the setting characteristics by interfering with the rate at which calcium and aluminum polyacrylates are formed [2]. The authors have previously investigated the use of tartaric acid, however, no observable difference was determined. It is also been suggested that Na^+ release from the commercial glass can initially neutralize the COO^-

groups from the PAA chain which are subsequently replaced by Ca^{2+} or Al^{3+} after a period of time [34]. The T_s observed for Fuji IX and Ketac Molar correlate well to those reported in the literature [8] and lie within the limits outlined by ISO9917 where a minimum of 90 s and a maximum of 360 s is required [24]. Determination of a material's setting exotherm (S_x Fig. 3b) is an important characteristic when developing orthopedic materials as contact with blood and other physiological organic components are critical to the healing process. The S_x of BT 101 was closer to body temperature ($A_T + 9$ °C) then either Fuji IX ($A_T + 4$ °C) or Ketac Molar ($A_T + 4$ °C) which is a positive attribute as elevated temperatures can have negative effects on bone and nerve cells and can induce coagulation of proteins [35, 36]. Studies by Crisp et al. found that the S_x of GPCs had the lowest of any biomedical cement, which contributes to these materials biocompatibility [6].

4.3 Mechanical properties

Compressive strength testing (σ_c) was conducted on each cement and is presented in Fig. 4a. It was determined that each cement (BT 101, Fuji IX, Ketac Molar) did not exhibit significant changes in σ_c with respect to maturation (Table 2). However, at each time period BT 101 was significantly lower than Fuji IX and Ketac Molar ($P = 0.0001$). Fuji IX and Ketac experienced σ_c over 1–90 days which correlate with previous findings by Higgs et al. [8] (Fuji IX) and McCabe and Nomoto [37] (Ketac Molar). There were also no significant changes in **biaxial flexural strength (σ_f)**, particularly regarding (Fuji IX and Ketac Molar) with respect to maturation (Fig. 4b; Table 3). However, it can be observed in Fuji IX and Ketac Molar that a maximum strength is achieved after 30 days and subsequently reduces after 90 days. This may be attributed to the strengthening mechanism employed by GPCs where strengthening has been attributed to an ongoing setting reaction where, after the material reaches a maximum strength, extensive crosslinking makes the material more brittle and sensitive to flaws [38]. A significant increase in strength was observed when comparing BT 101 1 day to 90 days ($P = 0.009$) which suggests that BT 101 may be

Table 2 Compressive strength means comparison with respect to maturation

	1 vs. 7 days	7 vs. 30 days	30 vs. 90 days
BT 101	1.000	1.000	0.052
Fuji IX	1.000	0.245	0.148
Ketac Molar	1.000	0.424	0.259

* Significant at $P \leq 0.05$

Table 3 Biaxial flexural strength means comparison with respect to maturation

	1 vs. 7 Days	7 vs. 30 Days	30 vs. 90 Days
BT 101	0.098	1.000	1.000
Fuji IX	1.000	1.000	1.000
Ketac Molar	1.000	1.000	1.000

* Significant at $P \leq 0.05$

Table 4 Biaxial flexural modulus means comparison with respect to maturation

	1 vs. 7 Days	7 vs. 30 Days	30 vs. 90 Days
BT 101	1.000	1.000	0.092
Fuji IX	1.000	1.000	1.000
Ketac Molar	0.932	1.000	1.000

* Significant at $P \leq 0.05$

increasing in strength over long time periods. When comparing BT 101 to Fuji IX at 7 ($P = 0.027$) and 90 ($P = 0.008$) days, no significant difference in σ_f was observed, suggesting BT 101 may have a tensile strength comparable to Fuji IX. Previous work on Ketac Molar by Pearson and colleagues [39] found similar σ_f values and also observed no significant change in strength over 1, 7, 30, and 90 days, also Higgs et al. [40] (Fuji IX) found comparable σ_f (53 MPa) to this study. The lower mechanical properties (σ_c and σ_f) associated with BT 101 is likely due to a lower cross-linked density when compared to Fuji IX and Ketac Molar. Aluminium ion in the commercial materials forms extensive crosslinking with COO^- groups from the PAA chains. In relation to BT 101, Ca^{2+} and Zn^{2+} principally form polycarboxylates, and the larger particle size associated with BT 101 may result in a reduction in the glass dissolution rate which greatly reduces the availability of Ca^{2+} and Zn^{2+}. This will result in a reduction in polycarboxylate formation between the metal cations and PAA, and will reduce the overall mechanical strength. However, particle dissolution over long periods of time may result in an increase mechanical strength. Regarding BT 101, Fuji IX, and Ketac Molar there was no significant difference in **biaxial flexural modulus (E_f)** with respect to maturation (Fig. 5a; Table 4). However, significant differences in E_f were determined when comparing BT 101 to Fuji IX and Ketac Molar at each time period, 1 day ($P = 0.001$, $P = 0.003$), 7 day ($P = 0.029$, $P = 0.001$), 30 days ($P = 0.018$, $P = 0.003$) and 90 days ($P = 0.001$, $P = 0.0001$), respectively. There was no significant difference between Fuji IX and Ketac Molar at each time period. Although statistically there was no significant change in E_f observed with Fuji IX and Ketac Molar, a trend can be observed with both materials where

Table 5 Hardness means comparison with respect to maturation

	1 vs. 7 Days	7 vs. 30 Days	30 vs. 90 Days
BT 101	1.000	0.001	0.000
Fuji IX	0.000	0.000	0.000
Ketac Molar	0.000	0.000	0.000

* Significant at $P \leq 0.05$

the E_f was found to increase from 1 to 90 days. This may be due to the dissolution of residual glass within the cement matrix facilitating an increase in Al–PAA cross-linking. Although the E_f of BT101 was observed to increase over 1–90 days from 0.39 to 0.55 GPa, this change was not found to be significant. **Hardness** values are presented in Fig. 5b and while Fuji IX and Ketac Molar showed little deviation, BT 101 showed a significant decrease over 1–90 days (Table 5).This may be related to the greater particle size of BT 101. Incomplete particle dissolution and large glass particles present in the GPC matrix could account for the increased hardness and particle dissolution over long periods of time could explain the overall reduction in hardness.

Glass polyalkenoate cements have mechanical properties which are satisfactory for dental applications; however, materials used in spinal surgery require properties similar to the host tissue, *i.e.* trabecular bone. It is evident that the Al present in the glass phase of the commercial GPCs significantly increases the mechanical properties. However, by modifying the glass composition, it is possible to alter the mechanical properties and setting characteristics of these materials. By including Zn and Sr in the glass phase, it has been possible to modify the properties to more closely suit spinal applications. The literature suggests that the σ_c of trabecular bone lies between 4 and 12 MPa, the modulus lies between 1 and 20 GPa [41, 42] which are significantly lower than the mechanical properties of the commercial GPCs and acrylic cements [43]. The mechanical properties of BT 101 are more closely suited to the surrounding tissue if used in spinal applications; however, the handling properties are the major drawback associated with this experimental material. The next step in this work is to determine the bioactivity of this experimental GPC against Fuji IX and Ketac Molar in relation to ion release, antibacterial properties, and cytocompatability as a function of time.

References

1. Tyas MJ, Burrow MF. Adhesive restorative materials: a review. Aust Dent J. 2004;49(3):112–21.

2. Nicholson JW, Wilson AD. Acid–Base cements — their biomedical and industrial applications. Chemistry of Solid State Materials. Vol. 3. 1993: Cambridge.

3. Nicholson JW. Adhesive dental materials—a review. Int J Adhes Adhes. 1998;18(4):229–36.

4. Smith DC. Development of glass–ionomer cement systems. Biomaterials. 1998;19(6):467–78.

5. Cho S, Cheng AC. A review of glass ionomer restorations in the primary dentition. J Can Dent Assoc. 1999;65:491–5.

6. DeBruyne MAA, DeMoor RJG. The use of glass ionomer cements in both conventional and surgical endodontics. Int Endod J. 2004;37:91–104.

7. Akinmade AO, Nicholson JW. Glass ionomer cements as adhesives. J Mater Sci Mater Med. 1993;4(2):95–101.

8. Higgs WA, Lucksanasombool P, Higgs RJED, Swain MV. Comparison of the material properties of PMMA and glass ionomer based cements for use in orthopedic surgery. J Mater Sci Mater Med. 2001;12:453–60.

9. Zimehl R, Hannig M. Non metallic restorative materials based on glass ionomer cements — recent trends and developments. Colloids Surf A: Physicochem Eng Asp. 2000;163(1):55–62.

10. Reusche E, Pilz P, Oberascher G, Linder B, Egensperger R, Gloeckner K, Trinka E, Iglseder B. Subacute fatal aluminium encephalopathy after reconstructive otoneurosurgery: a case report. Human Pathol. 2001;32(10):1136–9.

11. Hatton PV, Hurrell-Gillingham K, Reaney IM, Miller CA, Crawford A. Devitrification of ionomer glass and its effect on the in vitro biocompatibility of glass ionomer cements. Biomaterials. 2003;24:3153–60.

12. Polizzi S, Pira E, Ferrara M, Bugiani M, Papaleo A, Albera R, Palmi S. Neurotoxic effects of aluminium among foundry workers and alzheimers disease. Neurotoxicology. 2002;23: 761–74.

13. Weber A, May A, von Ilberg C. Bone replacement by ionomer cement in osteoplastic frontal sinus operations. Eur Arch Otorhinolaryngol. 1997;254(1):162–4.

14. Firling CE, Hill TA, Severson AR. Aluminium toxicity perturbs long bone calcification in the embryonic chick. Arch Toxicol. 1999;73:359–66.

15. DeMaeyer EAP, Verbeeck RMH, Vercruysse CWJ. Infrared spectrometric study of acid degradable glasses. J Dent Res. 2002;81(8):552–5.

16. Nicholson JW. Chemistry of glass ionomer cements. Biomaterials. 1998;19:485–94.

17. Yamaguchi M, Ma ZJ. Role of endogenous zinc in the enhancement of bone protein synthesis associated with bone growth of newborn rats. J Miner Metab. 2001;19:38–44.

18. Yamaguchi M, Ma ZJ. Stimulatory effect of zinc on Deoxyribonucleic acid synthesis in bone growth of newborn rats: enhancement with zinc and insulin like growth factor-I. Calcif Tissue Int. 2001;69:158–63.

19. Wren AW, Boyd D, Thornton R, Cooney JC, Towler. Antibacterial properties of a tri-sodium citrate modified glass polyalkenoate cement. J Biomed Mater Res B Appl Biomater. 2009;90-B(2):700–9.

20. Sawai J. Quantitative evaluation of antibacterial activities of metallic oxide powders (ZnO, MgO and CaO) by conductimetric assay. J Microbiol Methods. 2003;54:177–82.

21. Sawai J, Shinobu S, Igarashi H, Hashimoto A, Kokugan T, Shimizu M, Kojima K. Hydrogen peroxide as an antibacterial factor in zinc oxide powder slurry. J Biosci Bioeng. 1998;86(5):521–2.

22. Marie PJ. Strontium ranelate: new insights into its dual mode of action. Bone. 2007;40(5):S5–8.

23. Marie PJ. Strontium ranelate; a novel mode of action optimizing bone formation and resorption. Osteoporos Int. 2005;16:S7–10.

24. International Organization for Standardization 9917, Dental Water Based Cements (E), in Case Postale 56. 1991: Geneva, Switzerland. p. CH–11211.

25. Williams JA, Billington RW, Pearson GJ. The effect of the disc support system on biaxial tensile strength of a glass ionomer cement. Dent Mater. 2002;18:376–9.

26. Higgs WAJ, Lucksanasombool P, Higgs RJED, Swain MV. A simple method of determining the modulus of orthopaedic bone cement. J Biomed Mater Res (Appl Biomater). 2006;58:188–95.

27. Boyd D, Towler MR, Watts S, Hill RG, Wren AW, Clarkin OM. The role of Sr^{2+} on the structure and reactivity of SrO–CaO–ZnO–SiO_2 ionomer glasses. J Mater Sci: Mater Med. 2008;19: 953–7.

28. Stamboulis A, Law RV, Hill RG. Characterization of commercial ionomer glasses using magic angle nuclear magnetic resonance (MAS–NMR). Biomaterials. 2004;25(17):3907–13.

29. Van Duinen RNB, Kleverlaan CJ, de Gee AJ, Werner A, Feilzer AJ. Early and long-term wear of 'Fast-set' conventional glass–ionomer cements. Dent Mater. 2005;21(8):716–20.

30. Pascual B, Vazquez B, Gurrachaga M, Goni I, Ginebra MP, Gil FJ, Planell JA, Levenfeld B, Roman JS. New aspects of the effect of size and size distribution on the setting parameters and mechanical properties of acrylic bone cements. Biomaterials: Processing, Testing and Manufacturing Technology. 1996; 17(5):):509–16.

31. Kaplan AE, Williams J, Billington RW, Braden M, Pearson GJ. Effects of variation in particle size on biaxial flexural strength of two conventional glass–ionomer cements. J Oral Rehabil. 2004; 31:373–8.

32. Serra J, Gonzalez P, Liste S, Chiussi S, Leon B, Perez-amor M, Ylanen HO, Hupa M. Influence of the non-bridging oxygen groups on the bioactivity of silicate glasses. J Mater Sci: Mater Med. 2002;13:1221–5.

33. Wilson AD, Hill RG, Warrens CP, Lewis BG. The influence of Polyacid molecular weight on some properties of glass ionomer cements. J Dent Res. 1989;68(2):89–94.

34. Billington RW, Williams JA, Pearson GJ. Ion processes in glass ionomer cements. J Dent. 2006;34:544–55.

35. Bergmann G, Graichen F, Rohlmann A, Verdonschot N, van Lenthe GH. Frictional heating of total hip implants. Part 2: finite element study. J Biomech. 2001;34(4):429–35.

36. Deramond H, Wright NT, Belkoff SM. Temperature elevation caused by bone cement polymerization during vertebroplasty. Bone. 1999;25(2):17–21.

37. Nomoto R, McCabe JF. Effect of mixing methods on the compressive strength of glass ionomer cements. J Dent. 2001;29:205–10.

38. Azillah MA, Anstice HM, Pearson GJ. Long term flexural strength of three direct aesthetic restorative materials. J Dent. 1998;26(2):177–82.

39. Khouw-Liu VHW, Anstice HM, Pearson GJ. An in vitro investigation of a poly(vinyl phosphonic acid) based cement with four conventional glass ionomer cements. Part 1: flexural and fluoride release. J Dent. 1999;27:351–7.

40. Higgs WAJ, Lucksanasombool P, Higgs RJED, Swain MV. Evaluating acrylic and glass–ionomer cement strength using the biaxial flexure test. Biomaterials. 2001;22(12):1583–90.

41. Turner CH, Takano Y, Rho J, Tsui TY, Pharr GM. The elastic properties of trabecular and cortical bone tissues are similar: results from two microscopic measurement techniques. J Biomech. 1999;32:437–41.

42. Zioupos P, Currey JD, Hamer AJ. The role of collagen in the declining mechanical properties of aging human cortical bone. J Biomed Mater Res. 1998;45(2):108–16.

43. Boyd D, Towler MR, Wren AW, Clarkin OM. Comparison of an experimental bone cement with surgical simplex p, spineplex and cortoss. J Mater Sci Mater Med. 2008;19(4):1745–52.